

Evaluation of CO₂ in Saline Aquifers under Deep Ground Water Systems in Urumqi River Basin of Xinjiang, China

Maina John Nyongesah^{1,2}

¹ Department of Biological Sciences, Jaramogi Oginga Odinga University of Science and Technology, P.O Box 210, Bondo, Kenya

² State Key Laboratory of Desert and Oasis Ecology, Xinjiang Institute of Ecology and Geography, Chinese Academy of Science, 818 Beijing Road south, Urumqi, Xinjiang, 830011, China

* Corresponding author's email: jr_nyongesah@yahoo.co.uk

ABSTRACT

The future emissions of carbon dioxide (CO₂) are likely to increase beyond the current levels due to rapid industrialization in China. Several methods have been proposed as possible mitigation strategies to reduce the anthropogenically emitted CO₂ from the atmosphere and water. This study provided the description of stratigraphic structure of the basin through analysis between the regional groundwater flow and the injection of carbon dioxide. The geological and geomechanical data was used to model the aquifer for geostatistical analysis. Data storage sites for geotechnical provided critical information to assess the potential risks and associated sequestration. The movement of groundwater occurred slowly with infiltration through the pores. CO₂ was stored in deep aquifers for longer periods due to slow movement of water downstream. Over time, the injected CO₂ dissolved water, forming minerals through chemical reactions, which converted it into carbonate minerals resulting in permanent sequestration. The chemistry of formation waters in this basin is important for many geological processes, such as the fluid-rock interaction, the migrating paths of fluid and the entrapment mechanisms of hydrocarbon. In this study, the emissions of CO₂ were shifted several kilometers away from the storage area, such that the regional groundwater mixing affected the quality of surface water with consequent of toxicity to every living creature that depended on the available water from Urumqi River Basin. Injection of fluids into deep saline aquifers is therefore considered as the best mitigating strategy for CO₂ abatement in water due to its enormous storage capacity.

Keywords: CO₂ sequestration; saline aquifer; numerical simulation

INTRODUCTION

Deep formations (e.g., saline aquifers, oil and gas reservoirs, and coal-beds) offer opportunities for geologic carbon sequestration as a promising method to mitigate the adverse impacts of climate change (Celia et al., 2015; Bachu and Bennion, 2016). The processes of capturing carbon dioxide (CO₂) emitted from large point sources and depositing it in deep geological formations is known as Carbon Capture and Storage (CCS). Such sources include fossil fuel based power plants and industrial sources (Celia et al., 2015). CCS provides a possibility to cut emissions while maintaining the access to fossil fuel energy until sufficient

alternative energy sources exist and it is necessary for some process industries. Numerous studies have been conducted to assess the CO₂ storage capacity of China's numerous sedimentary basins (Kyle et al., 2006; Baojun et al., 2010; Li et al., 2009). Due to the rich Mesozoic–Cenozoic tectonic and stratigraphic history, China has a significant CO₂ storage potential (Li et al., 2015).

By the end of the 21st century, the atmospheric greenhouse gas CO₂ concentration (CO₂) is predicted to increase from the current 370 μmol·mol⁻¹ to 540–970 μmol·mol⁻¹, and reach 550 μmol·mol⁻¹ by 2050 and 750 μmol·mol⁻¹ by 2100 (IPCC, 2001). These increases in the concentrations of CO₂ and other greenhouse gases

will cause an increase in mean global temperature by 1–3.5°C and are likely to increase evapotranspiration and changes in regional precipitation (Rind et al., 1990; Kattenberg et al., 1996; Stag et al., 2014).

Sequestration of CO₂ in deep saline aquifers is feasible since the estimated storage capacity of saline aquifers is very large and CO₂ is easily accessible in the saline aquifer formation (Celia et al., 2015; Garcia, 2003). Although large-scale injection of CO₂ is safely trapped in suitable geological structures, pressure changes and brine displacement may affect shallow groundwater resources by increasing the rate of discharge into a lake or stream, or by mixing of brine into drinking water aquifers (Bachu and Bennion, 2006; Garcia, 2003).

The processes of migration and storage of CO₂ in deep saline aquifers depend on the characteristics of brine displacement by CO₂ (drainage) during injection (Garcia, 2003). The CO₂ disposed in aquifers may appear partly as a free phase and partly as CO₂ dissolved in brine (Bachu, 2008; Zerai, 2005). Normally, CO₂ exists in three different states (liquid, gas, and supercritical) depending on the pressure and temperature of deep saline aquifers (Audigane et al., 2007). Supercritical CO₂ behaves like a gas, filling all the available volume, but has a density that varies with pressure and temperature from less than 200 kg/m³ to more than 900 kg/m³ (Zerai, 2005; Audigane et al., 2007).

Injection of CO₂ is prone to multiphase fluid flow, pressurization fluid and changes in effective stress (Garcia, 2003). Additionally, solute transport and chemical reactions between fluids and mineral formation has been reported during CO₂ migration into deep ground water (Garcia, 2003; Zerai, 2005). Although numerous studies have addressed the long-term efficiency of structural trapping of CO₂ (Garcia, 2003; Zerai, 2005; Audigane et al., 2007; Alley et al., 2007), little is known about the large-scale pressure changes caused by injection of CO₂ into deep saline formations.

Deep saline aquifers provide the largest potential subsurface storage capacity for the injected CO₂. The three different forms of CO₂ respond to pressure and temperature in different ways (Zerai, 2005; Cole et al., 2000; Zoback et al., 2003; Bachu et al., 2003; Ranjith et al., 2012). Bachu et al. (2003) explains that the three mechanisms for storage/sequestration of CO₂ operate on different

time scales and have different degrees of permanency, while other studies have indicated that this is an extremely slow process (Gu et al., 2008; Ranjith et al., 2012; Li et al., 2009; Gunter et al., 2006; Kyle et al., 2006). Lower fresh brine is usually pushed upwards, giving rise to a fluid circulation mixing process that enhances the dissolution of free CO₂ gas in the fresh brine. This has been accelerated by sinking heavier CO₂-brine mixture vertically that displaces fresh brine (Anne and Yilian, 2010; Gunter et al., 2006; Baojun et al., 2010). Thermal properties permit the storage of CO₂ with higher density at shallower depths. Old foreland and continental basins are best suited for hydrodynamic trapping because they tend to be cold, stable, and close to hydrostatic pressure, as well as have erosion- or topography-driven, down-dip directed regional flow regimes (Gale, 2004; Dentz and Tartakovsky, 2008; Zerai, 2005).

Economically, the high cost associated with CO₂ capture, separation, compression, transportation and injection is another key hurdle. Globally, rapid deployment of CO₂ geological sequestration has been a major issue (Li et al., 2015). Some countries such as China have a large CO₂ storage capacity (Li et al., 2009; Li et al., 2015). This translates to over 90% of all the geological storage in both onshore and offshore sedimentary basins as well as continental deep saline aquifers. Despite this capacity, the major concern is to ensure that the injected CO₂ is well kept beneath the surface such that it will not have environmental effects or it will not leak into the atmosphere; therefore, suitability of the aquifers is of paramount importance.

In order to minimize the risk of leakage and also increase the effectiveness of CO₂ storage, the basin flow system should be deep and regional in scale, and driven by topography or erosion rebound. Faults, fractures, and unconformities are undesirable, because they may create pathways for CO₂ to migrate through the cap rock to the surface. In the presence of near horizontal confining layer and or relatively small density difference, the CO₂ will travel with the downward-directed regional groundwater flow (Bachu et al., 2003; Bachu, 2008). This can only be reversed with the presence of faults or other high permeability zones in the stratigraphic seal which provide escape routes to the surface. Therefore, the analysis of CO₂ injection using deep ground water systems is important in determining the suitability of the basin. This study focused on the

analysis of movement of CO₂ phase behavior and CO₂ migration including geochemistry and solid matrix deformation. This study was necessary to bridge the knowledge gap about basin groundwater hydraulics as well as recognize the cause and effect relation between regional groundwater flow and the phenomena (Zerai, 2005). Therefore, the aim of this study was to analyze the movement of injected carbon dioxide in deep saline aquifers based on deep groundwater systems.

MATERIALS AND METHOD

Study area

Urumqi River Basin (URB) (43°06'N, 86°49'E) is located in Xinjiang Uygur Autonomous Region. URB originates from Tianger peak at 4486 m above sea level. The river crosses the western part of Urumqi City, the capital of Xinjiang Uygur Autonomous Region, China and disappears in the desert. It is 53 km long with an average slope of 48.5%. Its physico-chemical characteristics are as follows; pH = 6.5–8.5; Eh = -125.3 mV; Nitrate <0.2 mg/L; Potassium = 0.18 mg/L; Ec = 390 μS/cm; Sodium = 36.2 mg/L; Sulfate = 1.8 mg/L; Magnesium = 21.3 mg/L; Manganese = 76.4 μg/L; Calcium = 13.2 mg/L; Copper = 3.5 mg/L; Arsenic = 360 μg/L; Cobalt = 0.09 mg/L; Aluminum = 57.67 μg/L;

Chromium = 78 μg/L; Iron = 125 μg/L. The river experiences an annual snowfall estimated at about 54% of the total precipitation. Its potential evaporation decreases with the increase in altitude. The lithology is primarily Siluric crystalline schist, with liberal amounts of gneiss, gabbro, granodiorite, granite, and quartzite (Li et al., 2011). Like the entire China, URB experiences a long winter period from the end of October every year to the end of March the following year; a spring period from April to end of May and a summer period from June to October. The mean annual temperature is estimated at - 5.4°C (Fig. 1), with mean temperatures below 0°C occurring from September to May.

Data collection

In this study, the goals that outlined the measures for the injection and storage of CO₂ were defined. Geology was characterized by the heterogeneity and uncertainty of the properties of CO₂ that is represented in aquifer models. On the basis of Lucier and Zoback (2008), an improved geo-mechanical model was developed for establishment of limits on injection pressures as well as evaluation of aquifer stimulation techniques. This was followed by the data collection in 3D aquifer models. This represents uncertainty of the aquifer attributes and heterogeneity that were constructed using geostatistics. The models were constructed

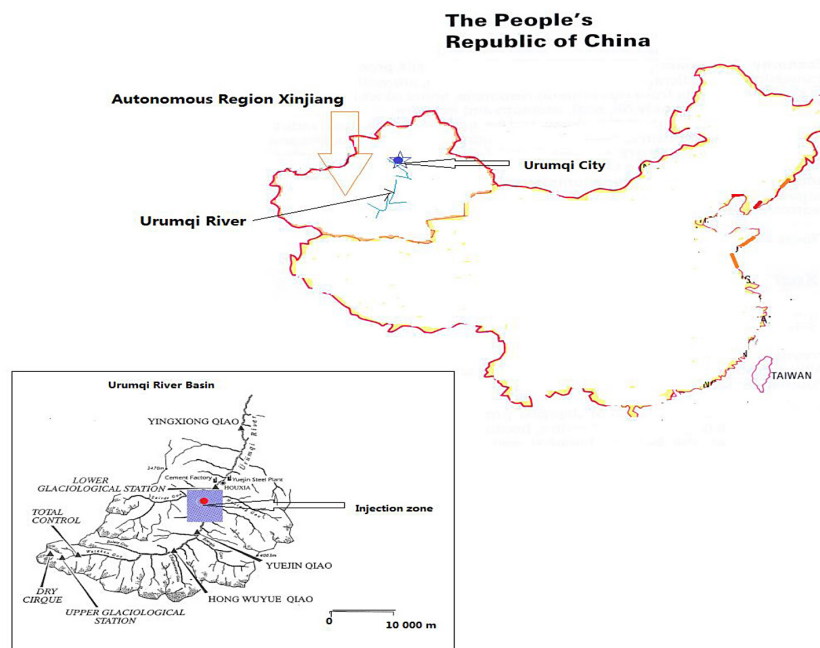


Figure 1. Study area location

finally before fluid flow simulations of CO₂ injection were run using the improved geomechanical constraints. This was carried out to the control injection pressures into groundwater.

Geological characterization and Soil Physical Characteristics of Urumqi River Basin

The data was collected at all the identified specific sites based on examination of hydrogeological properties of all of the aquifers. They were also characterized and all the existing natural fault and fracture systems were identified. Confirmation was done on the sealing caprock for each aquifer unity and characterization done on the risk of leakage through the caprock. A large part of the geological characterization was determined where property values were used to populate the 3D models.

Several aquifer properties were considered and they included; porosity, thickness, and permeability. The values ranged widely even within a single stratigraphic unit, particularly for the aquifers extending for hundreds of kilometers. Application of geostatistical methods in the 3D property modeling simulations led to estimation of both the distribution of the property values (Lucier and Zoback, 2008; Imaseki et al., 2005; Riaz et al., 2006).

Nutrient content

In each site, 6 samples of sediment were collected at 3 different depths ranging from 20, 40, and 60 cm to realize the spread of emission of Cardona in the ground in a river basin. The samples were collected twice from November 2010 (Start of winter) until April 2011 (early spring). In total, 12 samples spread over four sampling site per sampling date were collected.

Characterize the geomechanics

The background seismicity was characterized after consolidating regional and local geomechanical data. In order to determine the essential input into the fluid flow simulator, a full geomechanical characterization was provided for, which involved the initial formation pore pressures (P_p) and safe injection pressures. When hydraulic fracturing or injection induced micro-seismicity treatments were used, the caprock limited the safe injection pressure.

A full geomechanical analysis also provided the information for calculating whether the in

situ fracture network was hydraulically conductive. The feasibility of using horizontal injection wells and stimulation techniques that increase injectivity such as hydraulic fracturing and injection induced micro-seismicity for permeability enhancement was obtained after evaluation of the geomechanical characteristics. On the basis of several studies, the world Stress Map database was used to determine consistency of the state of stress at the local site and throughout the region of interest (Gunter et al., 2006; Kyle et al., 2006; Anne and Yilian, 2010). A fault was critically stressed as follows:

$$r \geq \mu(S_n - P_p) \quad (1)$$

where: (*r*) is the shear stress. It was important to resolve the fault plane as equal to or greater than the product of the effective normal stress,

(*S_n*) is the normal stress minus (*P_p*). This resolved on the fault plane and the coefficient of sliding friction (*μ*) along the fault plane.

P_p at which a fracture of a given orientation began to slip was referred to as the critical pore pressure *P_{critP}*, which is given by:

$$P_{critP} = \frac{S_n - r}{\mu} \quad (2)$$

Data Analysis

Geomechanics analysis

Calculation of Elastic Moduli

P- and S-wave velocity logs and the density log from the suite of geophysical were used to evaluate the Poisson's ratio and Young's modulus associated with different lithologies. Poisson's ratio (*v*) was calculated from the following relationship between the P-wave velocity (*V_p*) and the S-wave velocity (*V_s*):

$$v = \frac{v_p^2 - 2v_s^2}{2(v_p^2 - v_s^2)} \quad (3)$$

Young’s modulus (E) was then calculated from rock density (ρ), V_p , and ν :

$$E = 2\rho\nu^2(1 + \nu) \quad (4)$$

Vertical Stress Determination

Calculated the magnitude of S_v by integrating the density log throughout the depth of the well as follows:

$$s_v = \int \rho(z)gdz \approx \sum_{\rho_{avg}} g\Delta z \quad (5)$$

where: ρ is rock density, g : is gravity acceleration, z is depth, ρ_{avg} : is the average density and dz the depth interval

The magnitude of S_v was calculated by integration of rock densities from the surface to the depth of interest, z : In other words,

$$s_v = \int_0^z \rho(z)gdz \approx \rho(\text{mean})gz \quad (6)$$

Determination of Stress Orientation

As a well is drilled, stress was concentrated at the wellbore wall. This stress concentration was described by the well-known Kirsch equations. In a vertical well, the effective stresses at the wellbore wall were described as the hoop stress ($\sigma_{\theta\theta}$), the radial stress (σ_{rr}), and the stress parallel to the wellbore wall (σ_{zz}):

$$\begin{aligned} \sigma_{\theta\theta} &= s_{H\min} + s_{H\max} - 2(s_{H\max} - s_{H\min})\cos 2\theta - 2p_p - \Delta p - \sigma^{\Delta T} \\ \sigma_{rr} &= \Delta p \\ \sigma_{zz} &= s_v - 2\nu(s_{H\max} - s_{H\min})\cos 2\theta - p_p - \sigma^{\Delta T} \end{aligned} \quad (7)$$

where: θ is the angle around the hole measured from the azimuth of $S_{H\max}$, Pp is the pore pressure, ΔP is the difference between wellbore pressure (resulting from the weight of the drilling mud column) and Pp ; $\sigma^{\Delta T}$ is the thermal stress induced by cooling of the wellbore by ΔT degrees, and σ is the static Poisson’s ratio.

In a deviated well, the principal stresses acting in the vicinity of the wellbore wall were not aligned with the wellbore axis. Thus, the principal stresses were given by:

$$\begin{aligned} \sigma_{tmax} &= 1/2 \left(\sigma_{zz} + \sigma_{\theta\theta} + \sqrt{\sigma_{zz} - \sigma_{\theta\theta}^2 + 4\tau_{\theta z}^2} \right) \\ \sigma_{tmin} &= 1/2 \left(\sigma_{zz} + \sigma_{\theta\theta} - \sqrt{\sigma_{zz} - \sigma_{\theta\theta}^2 + 4\tau_{\theta z}^2} \right) \end{aligned} \quad (8)$$

Once steady state has been reached, the change in the hoop stress was calculated as follows:

$$\sigma_{\theta\theta}^{\Delta T} = (\alpha_t E \Delta T)/(1 - \nu) \quad (9)$$

Simulation of CO₂ injection

Interface irregularity can increase uncertainty in the storage capacity. This may lead to provision of extra local structural traps. On the basis of Figure 2, fluid flow simulations provided the information on realistic injection rates for injection well configurations and different aquifer properties. The region of significant pressure increased and extends far in the lateral direction much further than the limited extent of CO₂. Normally, the simulation runs cover a time period of 100 years altogether, comprising the 30-year injection period and a 70-year post-injection period. Though the characteristics of the sealing layer above the storage formation provide a safe structural trap for the CO₂, the seal permeability is high enough to allow for pressure changes throughout the sealing layer. The results were used to assess whether it was possible to achieve the storage goals of a study within defined economic controls. The goals of the project control how the simulations are set up. It is necessary to determine the time period for running the simulations. This includes deciding how long to inject the CO₂ and how long to monitor the plume after the injection stops. In most cases, the supply of CO₂ can be considered unlimited, such that the factor limiting the injection rate is the maximum safe bottom-hole pressure.

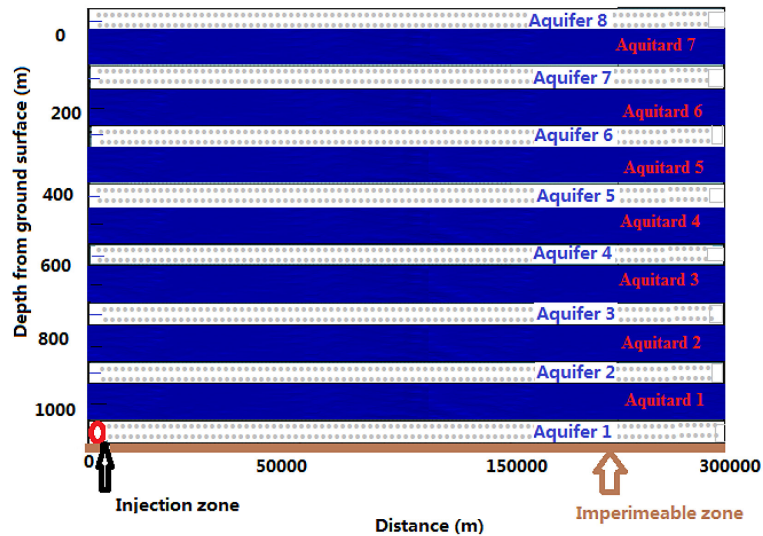


Figure 2. Schematic showing the CO₂ storage and overlying aquifer/aquitard sequence

RESULTS AND DISCUSSIONS

3D Model Stratigraphy

Saline aquifer formations represent the best salted sink for the storage of CO₂ among all geological options due to their enormous storage capacity (Li et al., 2015). Accurate description of stratigraphic structure of the basin is difficult due to topography despite the availability of information on basin’s geology and petroleum geology (Bachu and Bennionb, 2009). The obtained results show that the undulating fault development in the area (see Figure 3), caused severe deformation of the strata to be inclined. Essentially, the borehole data should be of approximately the same height. Even though there was interpolation, the actual surface interpolation surface did not match the phenomenon.

The Quaternary strata showed a thickening trend and the same trend from northwest to southeast but the cretaceous strata exhibited and

opposite trend thinning from the east to the west and also from north to south. The Jurassic stratum was thin in both ends of the basin but thicker in the middle of the east west direction. Additionally, it also showed a thickening trend from north to south direction. The Triassic, Permian and Carboniferous strata showed a thinning trend from west to east until they disappeared. All of the three strata also showed the same trend from north to south thinning out as they disappear. However, the Carboniferous stratum showed an interesting trend for both southeast – northwest and north. The south direction tended to thicken in the middle of the basin. It should be noted that because of the uneven distribution of drilling, some boreholes were drilled within the distribution of small structural units and this compromised the accuracy of determining formation structure.

Groundwater chemistry

Groundwater chemical characteristics are indicated in Tables 1 and 2. The pH values ranged

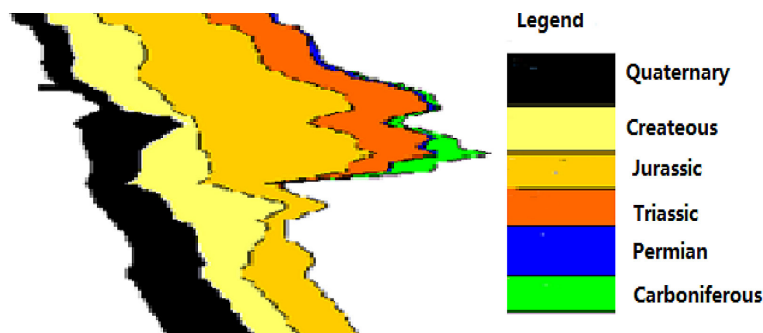


Figure 3. Model presentations of formations in the Urumqi River basin: disposition from Northwest to the Southeast

from 7.1 to 8.9, which may be due to high total salinity from wastewater and human activities in the basin. The geological formation in different water salinity varied significantly in the Urumqi basin. Lower Palaeozoic formation water salinity was lower in equilibrium compared to the Upper Paleozoic and Mesozoic formation water with the highest level of salinity at 100 g/L. The mean salinity in deep groundwater generally increased with depth as indicated in Table 1.

The difference in the salinity between the lower Palaeozoic formation, the Upper Paleozoic, Mesozoic and Palaeozoic strata was probably as a result of the sedimentary environment, jellyfish source conditions, lithology, temperature and water-rock interaction. Lower Paleozoic stratum developed in marine carbonate depositional environments and is buried deeper, which shows deep water circulation and good closed condition. This resulted in the original features of the residual water being saved. Additionally, the long process of historical development of the geological formation water led to high salinity levels (Harbison and Cox, 2002; Birkholzer et al., 2008). The Upper Paleozoic and Mesozoic strata waters have relatively low salinity which is a result of the shallow ground waters. The shallow ground water makes it vulnerable to surface water or meteoric water. The Lower Paleozoic formation water has a characteristic of high salinity, which can be attributed to its closed nature and the fact that it is buried enabling it to retain the characteristics of the original residual waters.

Table 1. Salinity means and pH values in all the formations

Depth	Formation	Salinity(g/)	pH
1	Shihezi	39.9	8.06
2	Yan an	45.6	7.37
3	Taiyuan	46.8	7.99
4	Majiagou	91.6	7.67
5	Shanxi	48.1	7.94
6	Yanchang	43.7	7.94

Therefore, geological development as well as long process of continuous enrichment and salt precipitation leads to high salinity.

The means of the formation waters of each group were used to study the general characteristics of the water quality of major strata. The means are shown in Table 2.

Within the river basin, the solutes that comprise more than 90% of all water solutes were bicarbonate (HCO_3^-), calcium (Ca^{+2} Ca), chloride (Cl), magnesium (Mg), potassium (K), sodium (Na) and sulfate (SO_4) (Table 2). Shihezi formation aquifer had groundwater pH value between 7.5 and 8.9, having an average of 8.06 which is less acidic. The formation has high levels of HCO_3^- and SO_4^{2-} , which shows significant levels of other ions. Extended group of water-bearing formation indicated that the hydrodynamic conditions are more complex, more groundwater sources, including rainfall recharge, compaction water and other sources of water having a fast local groundwater runoff.

The Yan'an groundwater had the pH values of 7.1 to 7.8 and an average of 7.37. The formation waters have high levels of K^+ , Na^+ and Cl indicating the formation in the entire extension of closure is favorable due to exposure of the surface area with high possibility of receiving recharge from precipitation.

The Taiyuan groundwater pH values ranged from 6.1 to 8.9 with an average of 7.99. The CO_3^{2-} content was negligible. All the other ions with the formation were of reasonable amounts indicating that the overall stone formation is closed from the local area outside the source water supplies.

The Majiagou groundwater pH values ranged from 7.1 to 8.5 with an average of 7.67 which is slightly acidic. All the ions except CO_3^{2-} were found in high levels but the levels of CO_3^{2-} were negligible. The formation is closed having a stagnated groundwater flow. In addition, the groundwater salinity is higher than seawater salinity.

Table 2. Ions composition means (g/L) and pH

Formation	pH	Chemical Compositions						
		K^+Na	Ca^{2+}	Mg^{2+}	Cl	SO_4^{2-}	CO_3^{2-}	HCO_3^-
Shihezi	8.06	9.3	3.9	0.2	20.6	0.3	0	1.2
Yan'an	7.37	10.3	1.5	0.3	14.2	3.5	0.1	1.1
Taiyuan	7.99	8.6	3.2	0.1	20.8	0.2	0.1	0.6
Majiagou	7.67	12.7	14.2	3.9	63.6	1.5	0	0.8
Shanxi	7.94	9.5	3.5	0.2	20.4	0.3	0.1	0.6
Yanchang	7.94	17.6	5.5	0.6	38.3	0.8	0.1	0.3

The Shanxi groundwater pH values ranged from 7.7 to 8.5 with an average of 7.94. Groundwater mineralization degree ranged from 9 to 89 g/L. The chemical composition of ground water in terms of Na^+ , Ca^{2+} , Cl^- and HCO_3^- were higher, while the CO_3^{2-} content was lower but local points were higher. This indicated that the overall closed Shanxi formation was good within all the local areas of surface or shallow groundwater recharge. Studies have indicated that sodium versus chloride ratios are good indicators of evaporation processes in ground water where evaporation increases the concentration of total dissolved solids.

The Yanchang groundwater pH values range from 7.3 to 8.8 and had an average pH of 7.94, which was alkaline. The CO_3^{2-} content increased significantly within the local point concentration while the other ions were in moderate amounts.

Characteristic indicators of formation water

The chemical composition of water from inflows is formed mainly by the dissolution of different types of salts caused by waters circulating in complicated systems of semipermeable rocks. Individual inflows are recharged by different flow systems, thus water/rock contact times are different. The basic hydrochemical ratios: sodium/chlorides ($r\text{Na}^+ / r\text{Cl}^-$), sulfides/chlorides ($r\text{SO}_4^{2-} \cdot 100 / r\text{Cl}^-$) and the carbonate equilibrium coefficient ($(r\text{HCO}_3^- + r\text{CO}_3^{2-}) / r\text{Ca}^{2+}$). The obtained results proved that hydrochemical ratios may serve as a supporting tool for better assessment of water threats in the basin. The chemical characteristic parameters of the formation water in this study were characterized by low sodium-chloride ratio ($r\text{Na}^+ / r\text{Cl}^-$). This could be residual formation water formed when gas was charged under a closed and reducing environment.

The sodium chloride ratio ($r\text{Na}^+ / r\text{Cl}^-$) reflects the degree of formation water and the concentration of metamorphic strata within hydrogeochemical environment. It is generally believed that the formation that are closed and more condensed with deeper metamorphism tend to have a smaller value of the $r\text{Na}^+ / r\text{Cl}^-$ ratio. This reflects the reduction of the water environment interaction. Lower Paleozoic of Urumqi River Basin, the Yanchang formation water reflected a lower $r\text{Na}^+ / r\text{Cl}^-$ ratio. Upper Paleozoic and Mesozoic strata had high values of $r\text{Na}^+ / r\text{Cl}^-$ ratio.

Carbonate equilibrium coefficient is a reflection of the strength parameters of the role of

de-carbonated. Lower Paleozoic Yanchang formation reflected a carbonate coefficient of 0.1. The geological formation of the Urumqi River Basin water chemistry changes in a comparative analysis of the composition in total salinity and water type for formations such as Shihezi and Taiyuan reflected high salinity with maximum in the basin. This implied that the water is in a closed alternating block structure in stagnation zone, with high total salinity, which is characterized by the long-term circulating of water – rock interaction in the formation.

Temperature characteristics

The temperatures (see Figure 4), however, tend to increase with depth having temperatures of slightly above 45°C. There are several formations in Northeast with a depth greater than 1000 m which also have a temperature of 40°C.

The Urumqi River Basin is not only a relatively independent groundwater system, but also low-temperature geothermal systems. The temperature is based on three vertically boreholes that had temperature values in the major strata as indicated in Figure 3. In this River Basin, the deep groundwater systems of depths 1000 m has a general temperature range of 30–40°C.

CONCLUSIONS

From this study, the density of supercritical CO_2 was lower than that of aqueous brine in the formation. This led to aquifer injected CO_2 to migrate rapidly upwards by buoyancy forces into the impermeable cap-rock. Gas spread horizontally within the cap-rock along impermeable rock even after halting of gas injection. Hydrodynamic trapping and solubility trapping occurred during the CO_2 injection phase, which increased the density of the CO_2 -brine mixture as it sunk downwards due to gravity.

Vertical permeability controlled fluid circulations in formation brine and CO_2 -brine mixture. This was important in the CO_2 solubility trapping and was only evident after hundreds of years. It was also evident that solubility trapping increased while gas trapping decreased over time. This was enhanced by continued brine CO_2 dissolution and gas trapping in the formation interstices between pores of the grains in the rocks.

By several years simulation time, saturation of separate phase CO_2 was expected to decrease to less than 2%. Most of the CO_2 in the source

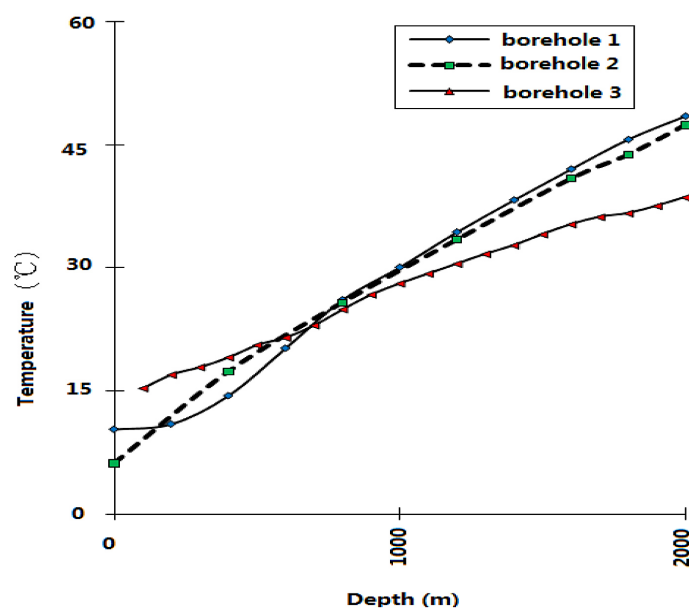


Figure 4. Temperature variations with depth

migrated away from the storage area and subsequently partitioned into solution in groundwater. Over the course of time, CO₂ (both separate and dissolved phases) migrated several km away from the storage area. No CO₂ was expected to reach the ground surface within 1000 years. It is proposed as a mechanism to safeguarding the quality of surface water and reducing the consequent water toxicity in the Urumqi River Basin.

Acknowledgements

This study was financially supported by the Knowledge Innovation project of Chinese Academy of science (KZCX2–YW–334). Many thanks goes to Prof Mupenzi Jean and Dr. Habiyaremye Gabriel for their helpful comments and excellent contribution to the improvement of this manuscript. Many thanks also to research team for assistance in the field work.

REFERENCES

- Celia M.A., Bachu V., Nordbotten J.M., Bandilla K.W. 2015. Status of CO₂ storage in deep saline aquifers with emphasis on modeling approaches and practical simulations, DOI: 10.1002/2015WR017609.
- Bachu S. & Bennion D.B. 2006. Dependence on Temperature, Pressure, and Salinity of the IFT and Relative Permeability Displacement Characteristics of CO₂ Injected in Deep Saline Aquifers. Society of Petroleum Engineers San Antonio, Texas, USA.
- IPCC. 2001. The scientific basis. In: Houghton J.T., Ding Y., Griggs D.J., Noguer M., Van der Linden P.J., Dai X., Maskell K., Johnson C.A., eds. Third assessment report of the Intergovernmental Panel on Climate Change”, Cambridge: Cambridge University Press.
- Rind D., Suozzo R., Balachandran N.K., Prather M.J. 1990. Climate Change and The Middle Atmosphere, Part 1: The Double CO₂ Climate. New York.
- Kattenberg A., Giorgi F., Grassl H., Meehl G.A., Mitchell J.F.B., Stouffer R.J., Tokioka, Weaver A.J., Wigley T.M.L. 1996. Climate models – projections of future climate, In Climate Change 1995: The Science of Climate Change, 285–357, (Eds J. T. Houghton, L.G.M. Filho, B.A. Callander, N. Harris, A. Kattenberg, and K. Maskell), Cambridge University Press, Cambridge, UK.
- Stag J., Mayr E., Koch H., Hattermann F.F., Huang S. 2014. Effects of Climate Change on the Hydrological Cycle in Central and Eastern Europe. In: Rannow S., Neubert M. (eds) Managing Protected Areas in Central and Eastern Europe Under Climate Change, Advances in Global Change Research, Springer, Dordrecht, 58. DOI: 10.1007/978-94-007-7960-0_3
- Garcia J.E. 2003. Fluid Dynamics of Carbon Dioxide Disposal into Saline Aquifers, University of California, Berkeley Nicholas Sitar, Chair.
- Bachu S. 2008. CO₂ storage in geologic media: role, means, status and barriers to Deployment. Progress in Energy and Combustion Science, 34, 254–273.
- Zerai B. 2005. CO₂ Sequestration in Saline Aquifer: Geochemical Modeling, Reactive Transport Simulation And Single-phase Flow Experiment. Trondheim, Norway.
- Audigane P., Gaus I., Czernichowski-Lauriol I., Pruess K., Xu T. 2007. Two-dimensional reactive transport modeling of CO₂ injection in a saline aquifer at the Sleipner Site, North Sea. American Journal of Science, 307, 974–1008.
- Gu W.Z., Seiler K.P., Stichler W. 2008. Transient response of groundwater systems to climate changes.

- Geological Society, London, Special Publications London.
12. Alley W.M., Reilly T.E., Franke O.L. 2007. Sustainability of Ground-Water Resources, General facts and concepts about ground water. U.S. Geological Survey Circular, 1186.
 13. Saylor B.Z. & Zerai B. 2004. Injection and Trapping of Carbon Dioxide in Deep Saline Aquifers, The Fossil Fuel Cycle Geological Society, London, Special Publications, 236(1), 285–296. DOI: 10.1144/GSL.SP.2004.236.01.17.
 14. Cole B.S., Baptist J., McPherson O.L. 2000. Multiphase CO₂ flow, transport and sequestration in the Powder River Basin, Wyoming, USA, Hydrology Program, New Mexico Institute of Mining and Technology, Socorro, NM 87801, USA.
 15. Zoback M.D., Barton C.A., Brudy M., Castillo D.A., Finkbeiner T., Grollmund B.R., Moos D.B., Peska P., Ward C.D., Wiprut D.J., 2003, Determination of stress orientation and magnitude in deep wells. *International Journal of Rock Mechanics and Mining Sciences*, 40, 1049–1076. DOI: 10.1016/j.ijrmms.2003.07.001
 16. Bachu S., Nordbotten J.M., Michael A.C. 2003. Injection and Storage of CO₂ in Deep Saline Aquifers: Analytical Solution for CO₂ Plume Evolution During Injection. Springer Publishers.
 17. Ranjith P.G., Perera M.S.A., Khan E. 2012. A study of safe CO₂ storage capacity in saline aquifers: a numerical study. *International Journal of Energy Research*, 37(3) DOI: 10.1002/er.2954
 18. Gunter W.D., Stefan B., Law D.H.S. 2006. Economic Feasibility of CO₂ Disposal in Aquifers within the Alberta Sedimentary Basin, Canada, T.J. McCann and Associates Ltd, Calgary, Alberta, Canada, T2P 3P4. Elsevier Science.
 19. Li X., Wei N., Liu Y., Fang Z., Dahowski R.T., Davidson C.L. 2009. CO₂ point emission and geological storage capacity in China. *Energy Procedia*, 1(1), 2793–2800.
 20. Kyle C.M., Robert H.W., Michael A.C. 2006. Opportunities for low-cost CO₂ storage demonstration projects in China, Department of Civil and Environmental Engineering, Princeton, NJ, USA.
 21. Anne N.O. & Yilian, L. 2010. Numeric modeling of carbon dioxide sequestration in deep saline aquifers in Wangchang Oil field-Jiangnan Basin, China. *Journal of American Sciences*, 6(8).
 22. Baojun B., Yang F., Tang D., Shari D.N., Wronkiewicz D. 2010. Characteristics of CO₂ sequestration in saline aquifers. China University of Petroleum (Beijing) and Springer-Verlag Berlin Heidelberg.
 23. Gale J. 2004. Geological storage of CO₂: What do we know, where are the gaps and what more needs to be done? *Energy*, 29, 1329–1338.
 24. Dentz M. & Tartakovsky D.M. 2008. Abrupt-interface solution for carbon dioxide injection into porous media. *Transport, Porous Med.* 51, 7, 1–13.
 25. Li X., Wei N., Liu Y., Fang Z., Dahowski T.R., Davidson L.C. 2009. CO₂ point emission and geological storage capacity in China. *Energy Procedia*, 1, 2793–2800.
 26. Lucier A. & Zoback M. 2008. Assessing the economic feasibility of regional deep saline aquifer CO₂ injection and storage: A geomechanics-based workflow applied to the Rose Run sandstone in Eastern Ohio, USA. *International Journal of greenhouse control*, 2, 230–247.
 27. Imaseki Y., Ohsumi T., Tomoda T., Uno M., Ohkuma H. 2005. Numerical simulation of the injection and migration behavior of carbon dioxide, in Proceedings of the 7th International Conference on Greenhouse Gas Control Technologies, Vancouver, 2181–2184.
 28. Riaz A., Hesse M., Tchelepi H.A., Orr F.M.Jr. 2006. Onset of convection in a gravitationally unstable diffusive boundary layer in porous media. *J. Fluid Mech.* 548, 87–111.
 29. Price J. & Smith B. 2008. Geologic storage of carbon dioxide, staying safely Underground, IEA Greenhouse gas R&D Programme.
 30. Lucier A., Zoback M., Neeraj G., Ramakrishnan T.S. 2006. Geomechanical aspects of CO₂ sequestration in a deep saline reservoir in the Ohio RiverValley region. The American Association of Petroleum Geologists/Division of Environmental Geosciences. American Geosciences.
 31. Pruess K., García J., Kovscek T., Oldenburg C., Rutqvist J., Steefel C., Xu T. 2004. Code intercomparison builds confidence in numerical simulation models for geologic disposal of CO₂”, *Energy* 29, 1431–1444.
 32. Nuth M. & Laloui L. 2008. Effective stress concept in unsaturated soils: Clarification and validation of a unified framework. *Int. J. Numer. Anal. Met.* 32, 771–801.
 33. Birkholzer J.T., Zhou Q., Tsang C.F. 2008. Large-scale impact of CO₂ storage in deep saline aquifers: A sensitivity study on pressure response in stratified systems. *Int. J. Greenhouse Gas Control*, 3(2), 181–194.
 34. Bachu S. & Bennionb D.B. 2009. Dependence of CO₂-brine interfacial tension on aquifer pressure, temperature and water salinity, Alberta Research Council Canada.
 35. Li L., Mupenzi J.P., Chen X., Achal V., Bao A., Habiyaemye G. 2011. Study on productivity of epilithic algae in Urumqi River Basin in Northwest China. *African Journal of Microbiology Research*, 5(14), 1888–1895. DOI: 10.5897/AJMR11.444
 36. Li P., Zhou D., Zhang C., Chen G. 2015. Assessment of the effective CO₂ storage capacity in the Beibuwán Basin, offshore of southwestern P.R. China. *International Journal of Greenhouse Gas Control*, 37, 325–339.
 37. Harbison J. & Cox M. 2002. Hydrological characteristics of groundwater in a subtropical coastal plain with large variations in salinity: Pimpama, Queensland, Australia. *Hydrological Sciences Journal*, 47(4), 651–665. DOI: 10.1080/02626660209492966